POR-2208(EX)
(WT-2208)(EX)
EXTRACTED VERSION

OPERATION SUN BEAM, SHOT SMALL BOY

Project Officers Report—Project 1.9

Crater Measurements

A. D. Rooke, Jr., Project Officer
L. K. Davis
J. N. Strange
U.S. Army Engineer Waterways Experiment Station
Vicksburg, MS

3 March 1965

NOTICE:
This is an extract of POR-2208 (WT-2208), Operation SUN BEAM, Shot Small Boy, Project Officers Report, Project 1.9.

Approved for public release; distribution is unlimited.

Extracted version prepared for
Director
DEFENSE NUCLEAR AGENCY
Washington, DC 20305-1000

1 September 1985

Destroy this report when it is no longer needed. Do not return to sender.

PLEASE NOTIFY THE DEFENSE NUCLEAR AGENCY ATTN: STTI, WASHINGTON, DC 20305-1000, IF YOUR ADDRESS IS INCORRECT, IF YOU WISH IT DELETED FROM THE DISTRIBUTION LIST, OR IF THE ADDRESSEE IS NO LONGER EMPLOYED BY YOUR ORGANIZATION.

UNCLASSIFIED

SECURITY CLASSIFICATION OF THIS PAGE

AD-A995 361

REPORT DOCUMENTATION PAGE

1a REPORT SECURITY CLASSIFICATION UNCLASSIFIED	1b RESTRICTIVE MARKINGS
2a SECURITY CLASSIFICATION AUTHORITY N/A since Unclassified	3 DISTRIBUTION/AVAILABILITY OF REPORT Approved for public release; distribution is unlimited.
2b DECLASSIFICATION/DOWNGRADING SCHEDULE N/A since Unclassified	
4 PERFORMING ORGANIZATION REPORT NUMBER(S)	5. MONITORING ORGANIZATION REPORT NUMBER(S) POR-2208 (EX) (WT-2208) (EX)
6a. NAME OF PERFORMING ORGANIZATION U. S. Army Engineer Waterways Experiment Station 6b OFFICE SYMBOL (If applicable)	7a. NAME OF MONITORING ORGANIZATION Defense Atomic Support Agency
6c. ADDRESS (City, State, and ZIP Code) Vicksburg, MS	7b. ADDRESS (City, State, and ZIP Code) Washington, DC
8a. NAME OF FUNDING/SPONSORING ORGANIZATION 8b. OFFICE SYMBOL (If applicable)	9. PROCUREMENT INSTRUMENT IDENTIFICATION NUMBER
8c. ADDRESS (City, State, and ZIP Code)	10 SOURCE OF FUNDING NUMBERS PROGRAM ELEMENT NO. / PROJECT NO. / TASK NO. / WORK UNIT ACCESSION NO.

11 TITLE (Include Security Classification)
OPERATION SUN BEAM, SHOT SMALL BOY, Project Officers Report—Project 1.9, Crater Measurements, Extracted Version

12 PERSONAL AUTHOR(S)
Rooke, A.D., Jr., Project Officer; Davis, L.K.; and Strange, J.N.

13a. TYPE OF REPORT	13b TIME COVERED FROM ____ TO ____	14. DATE OF REPORT (Year, Month, Day)	15. PAGE COUNT
		650303	73

16 SUPPLEMENTARY NOTATION This report has had sensitive military information removed in order to provide an unclassified version for unlimited distribution. The work was performed by the Defense Nuclear Agency in support of the DoD Nuclear Test Personnel Review Program.

17 COSATI CODES			18. SUBJECT TERMS (Continue on reverse if necessary and identify by block number)
FIELD	GROUP	SUB-GROUP	Sun Beam, Small Boy, Cratering, Crater Measurements
18	3		
19	4		

19 ABSTRACT (Continue on reverse if necessary and identify by block number)

The objectives of Project 1.9 were to obtain the dimensions of the apparent and true craters formed by the Small Boy event and to measure the permanent earth deformation occurring beyond the true crater boundary.

Measurements were made of the apparent crater by aerial stereophotography and ground survey and of the true crater and subsurface zones of residual deformation by the excavation and mapping of an array of vertical, colored sand columns which were placed along one crater diameter prior to the shot.

The results of the crater exploration are discussed, particularly the permanent compression of the medium beneath the true crater which was responsible for the major portion of the apparent and true crater volumes. Apparent and true crater dimensions are compared with those of previous cratering events.

20. DISTRIBUTION/AVAILABILITY OF ABSTRACT	21. ABSTRACT SECURITY CLASSIFICATION
☒ UNCLASSIFIED/UNLIMITED ☐ SAME AS RPT ☐ DTIC USERS	UNCLASSIFIED
22a NAME OF RESPONSIBLE INDIVIDUAL Mark D. Flohr	22b. TELEPHONE (Include Area Code) (202)325-7559 / 22c. OFFICE SYMBOL DNA/ISCM

DD FORM 1473, 84 MAR 83 APR edition may be used until exhausted. All other editions are obsolete.

SECURITY CLASSIFICATION OF THIS PAGE
UNCLASSIFIED

FOREWORD

Classified material has been removed in order to make the information available on an unclassified, open publication basis, to any interested parties. The effort to declassify this report has been accomplished specifically to support the Department of Defense Nuclear Test Personnel Review (NTPR) Program. The objective is to facilitate studies of the low levels of radiation received by some individuals during the atmospheric nuclear test program by making as much information as possible available to all interested parties.

The material which has been deleted is either currently classified as Restricted Data or Formerly Restricted Data under the provisions of the Atomic Energy Act of 1954 (as amended), or is National Security Information, or has been determined to be critical military information which could reveal system or equipment vulnerabilities and is, therefore, not appropriate for open publication.

The Defense Nuclear Agency (DNA) believes that though all classified material has been deleted, the report accurately portrays the contents of the original. DNA also believes that the deleted material is of little or no significance to studies into the amounts, or types, of radiation received by any individuals during the atmospheric nuclear test program.

OPERATION SUN BEAM

SHOT SMALL BOY

PROJECT OFFICERS REPORT—PROJECT 1.9

CRATER MEASUREMENTS

A.D. Rooke, Jr., Project Officer
L.K. Davis
J.N. Strange

U S. Army Engineer Waterways
Experiment Station
Vicksburg Mississippi

ABSTRACT

The Small Boy event

the device was detonated 10 feet above the playa of Frenchman Flat in the U. S. Atomic Energy Commission's Nevada Test Site. Measurements were made of the apparent crater by aerial stereophotography and ground survey and of the true crater and subsurface zones of residual deformation by the excavation and mapping of an array of vertical, colored sand columns which were placed along one crater diameter prior to the shot.

The apparent crater had an extrapolated depth of

A mound at ground zero reduced the depth at that point to 1.5 feet (~0.5 meter); however, this was not considered the apparent depth for comparison purposes. The true crater was and appeared to be coincident with the apparent crater in radial extent.

The results of the crater exploration are discussed, particularly the permanent compression of the medium beneath the true crater which was responsible for the major portion of the apparent and true crater volumes. Apparent and true crater dimensions are compared with those of previous cratering events, with emphasis on the range of burst heights above the surface.

DEFINITIONS

Apparent crater	The visible crater
Base surge	The low dust cloud, characteristic of a large explosion and most pronounced in an underground detonation. Surge begins near ground zero and propagates radially outward
Crater depth	Depth of the crater at ground zero as measured from the original ground elevation
Crater lip	The distinctly raised portion of the earth mass immediately surrounding an apparent crater
Crater radius	The average radius of a crater as measured horizontally from ground zero to its intersection with original ground surface
Height of burst (HOB) Depth of burst (DOB)	Distance above (below) original ground elevation (at ground zero) to the center of gravity of the explosive energy source

Ejecta (Throwout)	Material ejected from the crater by the force of the explosion
Elastic zone	The zone in which transient movement, but no permanent deformation, of the medium occurs
Fallback	The material between the true and apparent crater boundaries
Ground zero (GZ)	That point on the ground surface directly above or below the center of the energy source (the epicenter, or hypocenter, of the explosion)
Plastic zone	The zone in which the medium surrounding a crater has been permanently displaced (has flowed plastically), but in which there is no visible rupture or significant shear
Rupture/shear zone	The zone of material surrounding a crater which is characterized by fracturing and shearing, as well as by plastic movement
True crater	The crater prior to fallback

CONTENTS

CHAPTER 1

INTRODUCTION

1.1 OBJECTIVES

The objectives of Project 1.9 were to obtain the dimensions of the apparent and true craters formed by the Small Boy event (a low-airburst nuclear explosion) and to measure the permanent earth deformation occurring beyond the true crater boundary.

1.2 BACKGROUND

Since 1950, considerable effort has been directed toward developing a quantitative explanation of the various mechanisms that contribute to the formation of explosion-induced craters, as such craters have both military and civil significance. The apparent crater (see Figure 1.1) may represent a tactical obstacle or a planned excavation. The true crater is an indicator of the portion of the explosive energy which actually contributed to crater formation; for nuclear bursts at the surface, this quantity has been estimated to be approximately 2 percent of the total explosive energy (Reference 1). Knowledge concerning the zones

underlying the true crater, which exhibit varying degrees of deformation, is primarily of importance in the prediction of damage to underground military targets.

Several methods have been employed to define and measure the various regions of earth disturbance in land craters. For large craters, the most successful method has utilized colored sand columns vertically embedded in the earth near ground zero (GZ) (Reference 2). Thus, permanent movement of the medium outside the limits of the true crater is reflected in the deformation of the columns and can be measured after excavation of the columns. Using this technique, the U. S. Army Ordnance Ballistics Research Laboratory, the U. S. Army Engineer Research and Development Laboratories, the Naval Ordnance Laboratory, and the Waterways Experiment Station (WES) have conducted tests to define the mechanics of crater formation. With the exceptions of Teapot Ess and Little Feller II (both nuclear detonations) and the Canadian high-explosive (HE) shots, these studies have been on a small scale. Neither these nor other experiments have permitted the formulation of a general, quantitative explanation of the phenomena involved, and crater prediction for large yields remains an inexact science

based upon empirical approaches. This is due largely to the many variables involved, as well as to the lack of data in some areas, particularly in connection with the cratering capabilities of near-surface explosions. The Small Boy event afforded the opportunity for measurements of a crater resulting from a low-yield nuclear explosion occurring immediately above a surface of homogeneous lacustrine silt.

The value of a cratering study such as Project 1.9 lies not only in the recording of a specific cratering event, but also in the application of the experimental results to the general problem of cratering; i.e. it is important not only to record what occurred under a fixed set of conditions but also to attempt to understand the various mechanisms involved in the gross phenomena.

1.3 THEORY OF CRATERING MECHANICS

Project 1.9 included no measurements of the explosive forces (i.e. pressures, ground motion, etc.) involved in the Small Boy cratering event; therefore, very little information of this nature, other than those parameters that can be estimated on the basis of data from previous effects

studies, was available to the authors at the time of this writing. However, in order that the reader may better understand the formation of the crater, a brief qualitative discussion of the basic theory of cratering mechanics (References 3 through 5) is presented herein. For better correlation with the Project 1.9 data, this discussion is presented in terms of the causes of crater formation, particularly for a nuclear explosion, rather than in terms of the energy partitioned into crater formation.

1.3.1 Plastic and Elastic Compression. A nuclear device exploded in direct contact with a soil or rock medium creates great initial shock and pressure due to the proximity of dense material (device case and surrounding medium) which absorbs a portion of the thermal and radiant energy of the explosion. This material then, by vaporization and expansion, converts most of the absorbed energy into mechanical force which is exerted upon the surrounding medium. The intense shock pressure diminishes rapidly for a wholly or partially confined explosion due to the large, almost instantaneous expenditure of energy on the medium proper and to its spherical divergence.

In an explosion above the ground surface, the

airspace between the device and the ground surface has a great effect on the transmission of the explosive energy to the medium and, consequently, greatly affects the process of crater formation. When a nuclear device is detonated in air, the only material immediately available to absorb the thermal energy of the explosion is the mass of the device itself and the relatively low mass of the surrounding air. Therefore, a considerable portion of the explosion energy escapes as heat, light, and nuclear radiation. The remaining energy is transmitted ultimately as mechanical force, i.e. the intense shock wave and the kinetic energy of particles that are set in motion.

In addition, the intervening airspace in a low airburst acts as a buffer between the device and the ground surface, in contrast to the direct energy coupling that is present when the device is in contact with the medium. This buffering action not only reduces the energy transmitted to the medium but also distributes the shock and pressure over a wider area of ground surface.

The most extensive region of soil deformation is defined by the limit of perceptible elastic deformation. When the blast energy reaches this region, its peak has

diminished to such an extent that the compressive stress exerted upon the medium can only deform the soil elastically. This deformation occurs primarily in the direction of stress-wave propagation.

Above the elastic zone lies the zone of plastic deformation. The compressive stress induced by the blast energy within this zone retains sufficient force to exceed the elastic limit of the soil and deform it plastically. In plastic failure, the soil usually flows away from the burst and permanently compresses in the direction of the applied stress.

Finally, the maximum effect of the shock and pressure of the explosion occurs in the zone of rupture and shear. Within this zone, the medium is crushed and sheared by the extreme compressive stresses exerted upon it. Although this region of rupture and shear constitutes a major portion of the volume enclosed within the envelope of permanent deformation for an underground explosion, it is usually considered to be relatively minor in a crater formed by an airburst. Depending upon burst geometry, it is probable that this zone is not always continuous, but may consist of a badly fractured region near the true crater, while in the

region beyond the plastic zone, shearing seems to predominate.

1.3.2 Ground Spall. Ground spall occurs as a result of the shock or compression wave; however, it does not involve a failure or deformation by compressive stress but rather by tensile stress. In a subsurface explosion, the shock-pressure wave travels upward until it encounters the air-ground interface and a rarefaction, or negative stress wave, develops. In the area near the ground surface, the rarefaction may be sufficiently intense to exceed the overburden stress and tensile strength of the medium so that the soil is ruptured along a plane normal to the direction of the stress-wave propagation and may even become completely dissociated and fly into the air (Reference 5).

A phenomenon akin to this probably occurs when the device is detonated above the surface. Here, however, the spalling results from sufficiently strong elastic rebound forces which dissociate the material.

1.3.3 Thermal Effects. Since a nuclear explosion is characterized by a very high energy-density ratio, a large percentage of the initial energy is released as thermal radiation. If the detonation is below the ground surface,

the entire surface area of the fireball encounters dense material which absorbs a portion of the thermal energy, and as a result, this material is itself liquefied or vaporized in the process.

In a surface or low airburst, only a portion, or, in some cases, none of the fireball encounters the soil medium, depending on the radius of the fireball and the height of burst (HOB). Thus, the amount of thermal energy absorbed by the medium depends upon the thermal conductivity properties of the medium itself, the area of the medium exposed, the fireball temperature, and the duration of the exposure. It seems probable, however, that very little of the crater volume resulting from a low airburst can be attributed to vaporization of the soil.

1.3.4 Ejecta (Throwout). In the deeper subsurface cratering events, the expanding gas bubble imparts considerable momentum to the particles of the medium which it encounters as it expands and rises. For most cratering events, the expanding bubble (with its accompanying scouring action) is the primary force involved in the removal of material from the true crater.

In a near-surface or low airburst, in addition to the

scouring effect of the expanding gases, some dissociated material is sucked up by the thermal updraft that is created when the superheated gases begin to rise and cooler air rushes in to fill the void (Reference 6). This process is probably aided by the rebound spalling mentioned in Paragraph 1.3.2. The amount of dissociated material that is deposited within and without the crater limits depends upon the burst geometry and the ambient winds. An associated phenomenon, the base surge aided by ambient winds, may also transport airborne particles in significant quantities beyond the crater.

1.4 CRATER-PREDICTION METHODS

No theoretical approach has yet been advanced which quantitatively explains the entire mechanism of the crater-formation process sufficiently to permit accurate predictions of crater dimensions.

The most widely recognized empirical solution to the problem of crater prediction involves the scaling of crater parameters in proportion to some fractional exponent (most often the cube root) of charge weight. This cube-root scaling, a derivative of Mach's law of similitude

(Reference 7), is valuable in modeling explosion effects; however, its validity and accuracy are questionable when cube-root scaling is applied to phenomena wherein the force of gravity is important or where extrapolations are attempted through several orders of magnitude to extreme ranges of charge yields. Basically, this method assumes that small craters are models of large craters, an assumption that is not entirely supported by theory or by experimental evidence. Several logical reasons have been advanced to explain the limitations of cube-root (and other exponential) scaling. Foremost among these is the fact that two laws of similitude are involved, viz., Froude's and Mach's. These cannot be simultaneously satisfied, and neither can be neglected. Briefly, Froude's law recognizes the acceleration due to gravity as the dominant factor in modeling, while Mach's law considers the compressibility of the media involved to be dominant; selection of either law automatically invalidates the scaling relations of the other. Where different explosives are involved (i.e. HE and nuclear), the differences in rates of detonation, energy densities, thermal effects, etc., cannot be ignored. Scaling according to Mach's law, however, requires that all such

physical properties be identical. Additionally, soil composition, strength, and increase in lithostatic (overburden) pressure with depth undoubtedly exert an influence on the shape of an explosion-produced crater. A thorough discussion of the independent variables involved in crater formation is presented in Reference 4.

As early as 1954, a scaling law for crater depth was suggested which advocated the use of an exponent of the charge weight intermediate to the commonly used fourth-root and cube-root laws for cratering in shallow water (Reference 8). The value most nearly representative of all experimental evidence available at that time appeared to lie between 1/3.5 and 0.3.

Additional and more recent experimentation has lent considerable credence to a variation of the classical cube-root scaling law, i.e. that of $Y^{1/3.4}$-scaling, where Y represents device yield in kilotons. A discussion of this and other scaling relations is contained in Reference 9, while certain theoretical support is offered in Reference 10, which indicates that 1/3.4-scaling may remain applicable even into the very high energy range ($Y \geq 10$ Mt). $Y^{1/3.4}$ scaling has been adopted in this report as a means of

expressing crater parameters as a function of yield.

A review of the theoretical literature on the subject of cratering, coupled with a comparison with observed results (as in Reference 5), reveals at once the many areas of uncertainty concerning this phenomenon. Probably nowhere are these uncertainties more pronounced than in the regime of airbursts, where the effects of energy coupling and the behavior of the cratered medium are only partially understood.

Because of the unavailability of an expressive theory and the present limitations of crater prediction, full-scale nuclear tests such as the Small Boy event provide the most dependable means of furthering the state of the art.

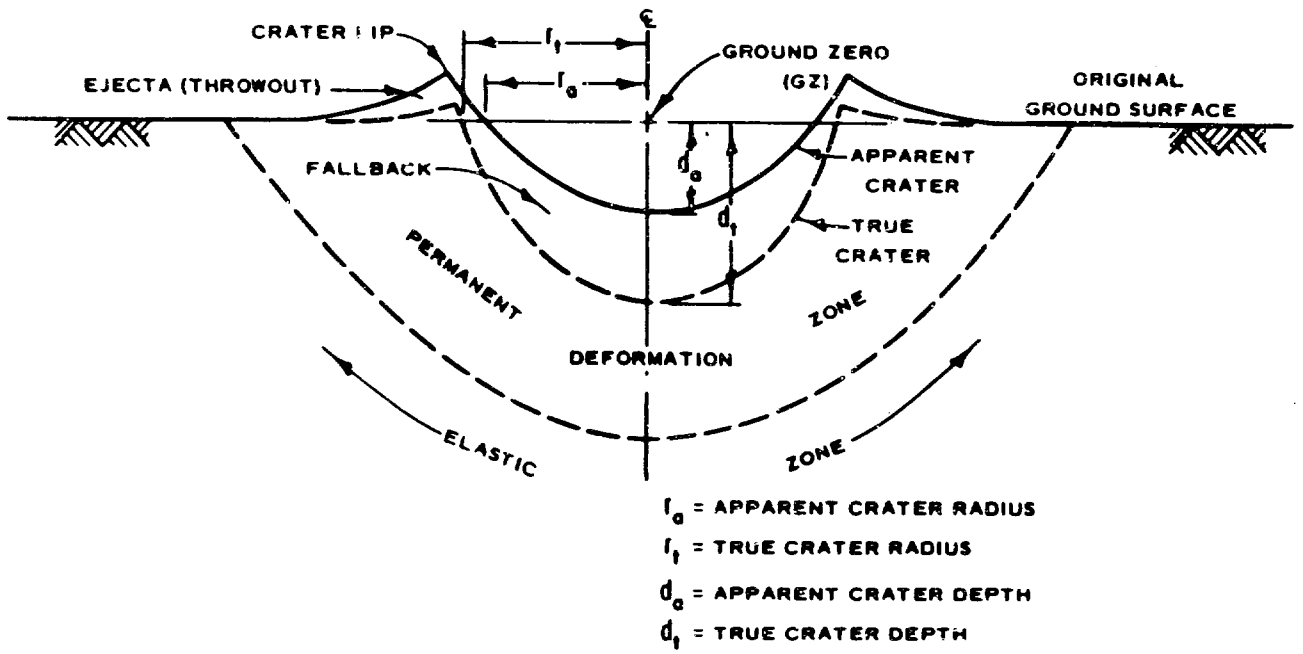

Figure 1.1 Idealized profile of a typical crater resulting from near-surface burst.

CHAPTER 2

PROCEDURE

2.1 SITE LOCATION AND TEST CONDITIONS

The site of the Small Boy event was the dry lake bed of Frenchman Flat in Area 5 (Figure 2.1) of the Atomic Energy Commission's Nevada Test Site (NTS).

The device was detonated at 1130 hours on 14 July 1962,

Weather conditions at firing time were clear and warm, with a 6-mph wind blowing from the southwest (225 degrees). Figure 2.2 shows selected photographs of the detonation.

2.2 CRATER PREDICTION

To insure an experimental array sufficiently extensive to reflect all required data, a prediction of the crater dimensions was made, based largely upon unpublished cratering curves available at WES. Predicted dimensions were as follows:

Apparent crater radius (r_a)

Apparent crater depth (d_a)

Little difference was anticipated between true and apparent crater dimensions. No predictions were made of the extent

of the rupture and plastic zones, but sand-column depths of 40 feet near ground zero were considered sufficient to provide the desired data. The Small Boy shot geometry and predicted crater dimensions are illustrated in Figure 2.3.

2.3 EXPERIMENTAL ARRAY

2.3.1 Geometry of Array. The experimental array consisted of 18 colored sand columns, each 8 inches in diameter and varying in depth from 10 to 40 feet. The columns extended outward from ground zero along two radials (a single diameter) a distance of 120 feet. Figure 2.4 shows the layout of the array, which was designed to provide the basis for measurements of the true crater and of the rupture and plastic zones along one crater diameter.

2.3.2 Preparation of Sand Columns. Holes for the sand columns were drilled by a truck-mounted, rotary-drill rig with hydraulic feed; the rig was operated by WES personnel. Locations for the holes were determined by a survey crew of the on-site contractor, Holmes and Narver. Soil characteristics at Frenchman Flat are such that vertical cuts are stable; hence, no difficulty was experienced from sloughing of boreholes during drilling operations. The sand columns

were formed by backfilling the holes with a mixture designed to closely match the strength and density of the surrounding medium. The mixture consisted of vegetable dye, lime, washed sand, and water in approximate proportions 1 (pound): 2 (sacks):0.8 (cubic yard):3 (gallons). As the mixture for a particular column was prepared, it was shoveled into the hole and tamped. At predetermined vertical intervals, varying from about 2 to 5 feet, a layer of asphalt cold mix was added in the required amount to give a tamped thickness of about 0.1 foot. Elevations to these asphalt layers were determined by readings taken on the graduated tamp, fitted with detachable handle sections for ease of use. This procedure was intended to give postshot indications of vertical, as well as horizontal, movement of the columns.

2.4 EARLY POSTSHOT CRATER MEASUREMENTS

Due to a high level of residual radioactivity, early postshot crater measurements were restricted to aerial stereophotographs taken by American Aerial Surveys, Inc., through an arrangement with Holmes and Narver. For this purpose, a Cessna 180 aircraft mounting a Park camera with a 6-inch focal length and distortion-free lens was used.

The Estar-base film was developed by the Department of Defense Continental Test Organization at Mercury, Nevada. Flight altitudes were 1,200 and 1,500 feet, and ground speed of the aircraft was about 80 mph. These rather high altitudes were necessary because of thermal turbulence common in this area during the summer. For ground reference, 16-by-18.5-foot concrete crosses formed from roof-shaped parking curbs had been placed before the shot at known locations and elevations. Postshot photography was accomplished on D+2 days. Negatives of the aerial photographs were sent to consulting engineers, who prepared an aerial map of the crater. Comparison with preshot aerial photographs (also made by American Aerial Surveys, Inc.) permitted evaluation of the crater dimensions.

2.5 LATER MEASUREMENTS OF APPARENT CRATER

It was planned that a conventional survey of the Small Boy apparent crater would be made when radioactivity levels at ground zero permitted. Just before the surface was judged safe, however, the ground surface in the immediate area of ground zero was disturbed to such an extent by work on another project that no worthwhile information could be obtained by surveying in the vicinity of ground zero. A ground surface profile was later surveyed along the axis of the sand columns in order to check the extent of the apparent crater as indicated by the aerial maps.

2.6 EXCAVATION OF SAND COLUMNS

Radioactivity levels had decayed sufficiently to permit work in the crater area by April 1963, and work on the excavation of the sand columns was begun. Excavation and measurement of the sand columns were accomplished by WES personnel with the use of equipment and labor supplied by Reynolds Electrical and Engineering Co., on-site contractor for the Atomic Energy Commission.

2.6.1 Excavation Procedure. Earth-moving equipment used for various stages of excavation included a 1-1/2-cubic-yard backhoe, a 50-ton crane with clamshell a TD-25 bulldozer, a front-end loader, and in the later stage of excavation, a pneumatic shovel. The bulldozer was used to scrape off 3 or 4 inches of contaminated ground surface before excavation began in an effort to minimize the radiation dosage which personnel would accumulate.

The excavation trench was dug about 1 foot from the line of columns on the southwest side. The excavation was conducted in two stages: (1) a trench 10 to 20 feet deep by 4 to 8 feet wide was cut by the backhoe along the length of the column array (Figures 2.5 and 2.6), and (2) the crane with a clamshell bucket was utilized to dig to the lower portions of the columns located 5 and 10 feet on either side of ground zero, down to a depth of 35 feet (Figures 2.7 and 2.8). The pneumatic shovel was used to complete the job.

As soon as the portion of the trench adjacent to a column was dug, the column was exposed along its entire depth by hand labor (Figures 2.9 and 2.10). In the deeper excavation at ground zero, however, the soil was too hard to permit exposure of the complete column below a depth of 20 feet. A pneumatic shovel was employed to tunnel into the trench wall until the asphalt layers were located.

2.6.2 Measurement of Sand-Column Displacement. Control for the measurement of sand-column movement consisted of four stations located 200 and 500 feet on each side of ground zero on the line of sand columns, and was established prior to the excavation by Holmes and Narver. The displaced positions of the sand columns were measured and recorded by the WES survey party using conventional surveying methods. The postshot positions of the columns were then plotted and compared with the preshot positions to determine the total horizontal and vertical displacement. In addition to displacement measurements, the extent of fracturing and general appearance of the columns were noted and recorded during the survey.

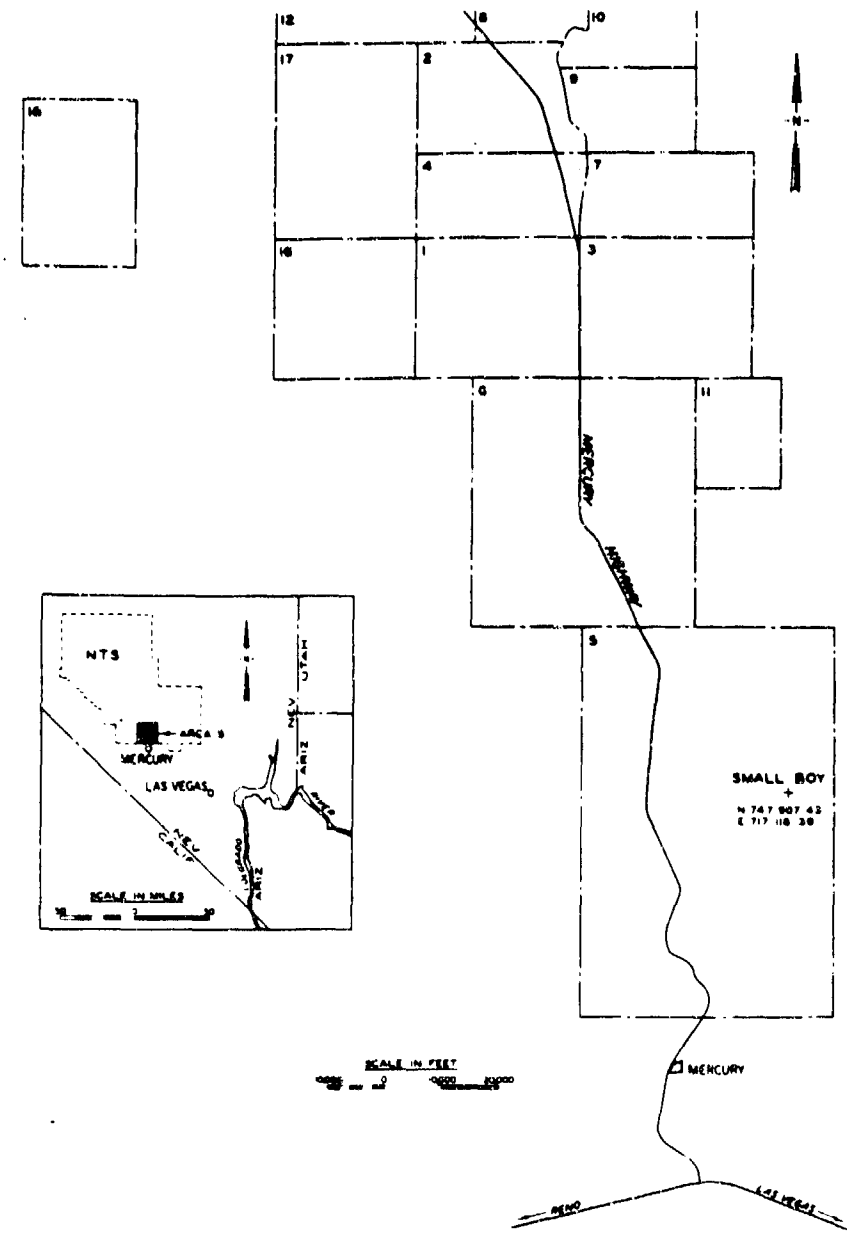

Figure 2.1 Nevada Test Site vicinity map. Nevada state coordinates are given for Small Boy GZ.

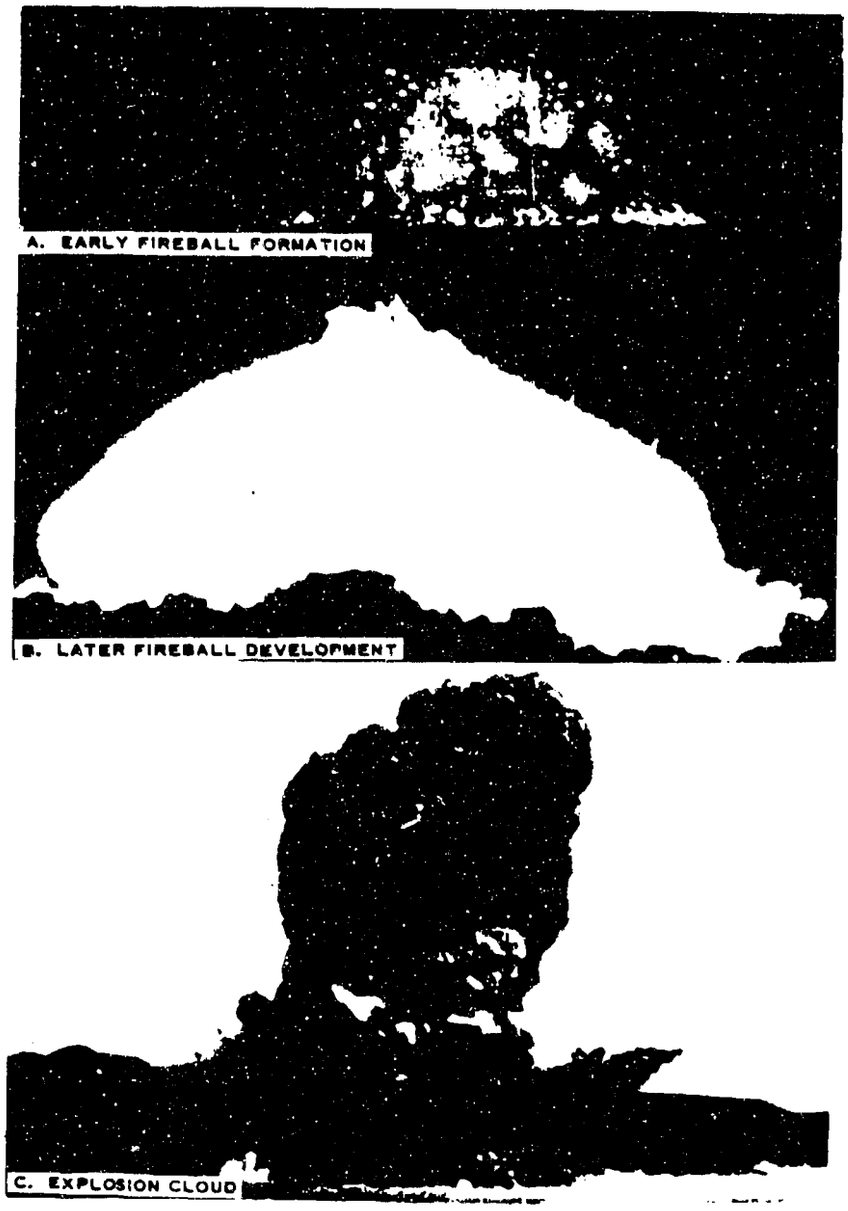

Figure 2.2 Small Boy detonation. (EG&G photo)

Page 34 Deleted

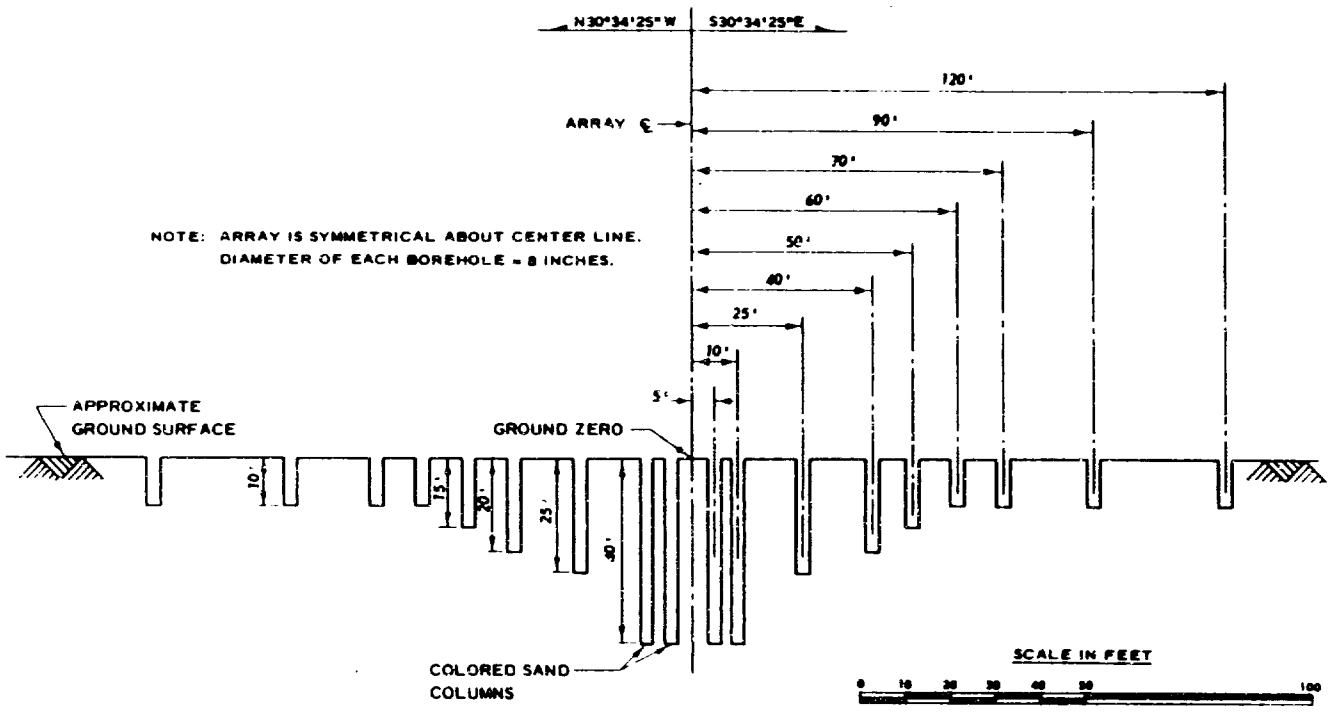

Figure 2.4 Sand-column array.

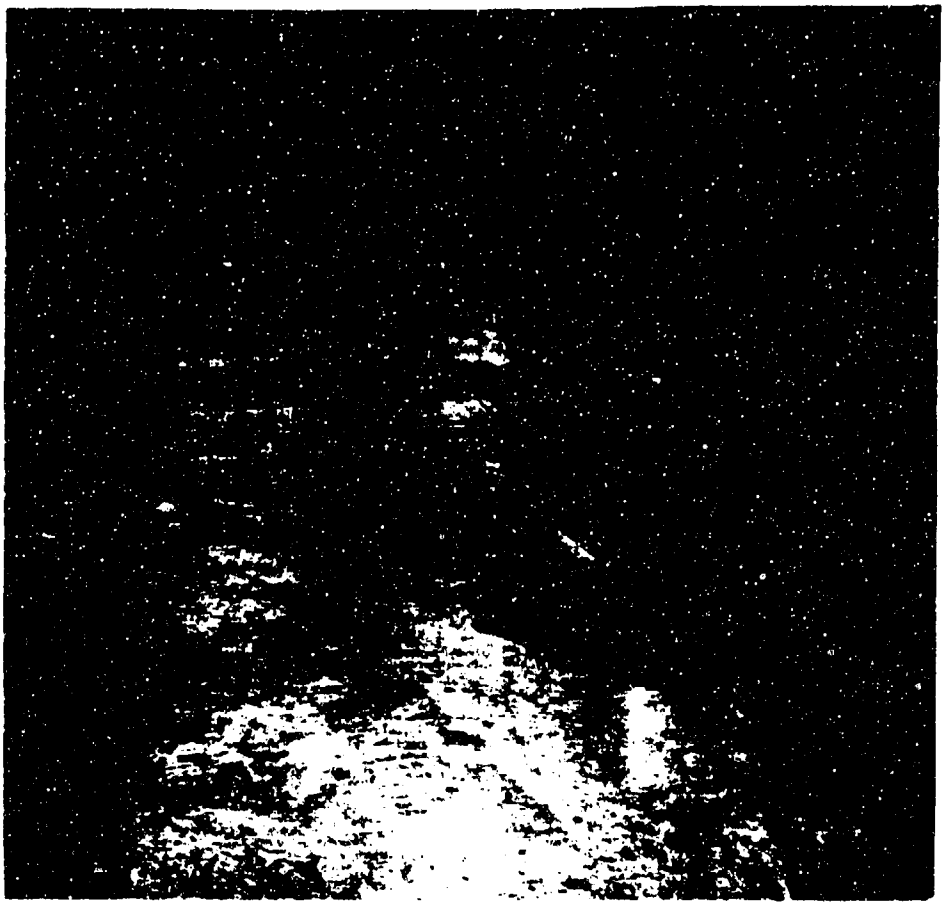

Figure 2.5 Backhoe cutting excavation trench along sand-column array. (WES photo)

Figure 2.6 Completed first stage of excavation trench. Man in bottom of trench is near GZ. View is looking north 31 degrees west. (WES photo)

Figure 2.7 Second stage of excavation. Crane with clamshell bucket excavating to lower portions of columns near GZ. The trench was widened at the top here to prevent loose fallback material in true crater from falling into working area 35 feet below. **(WES photo)**

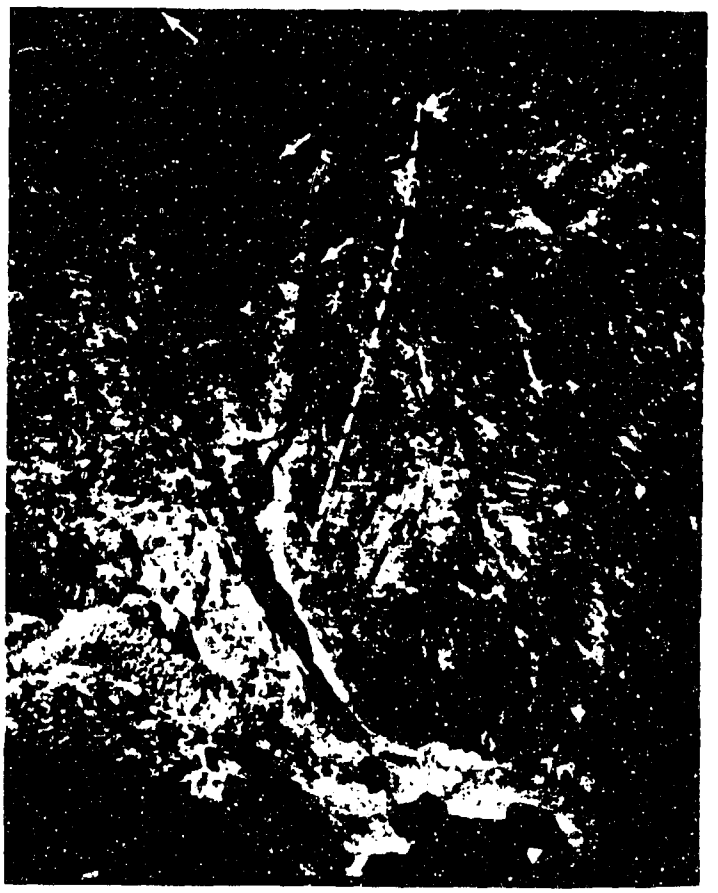

Figure 2.8 Completed second stage of excavation trench. Dotted line shows center point of trench wall, i.e. directly beneath GZ. Arrows indicate sand columns with upper portions exposed. Arrows from left to right indicate 25, 10, and 5 feet north of GZ, and 5 and 10 feet south of GZ. Note loose shalelike material within true crater at upper right. Bottom of trench is approximately 36 feet below original ground surface. **(WES photo)**

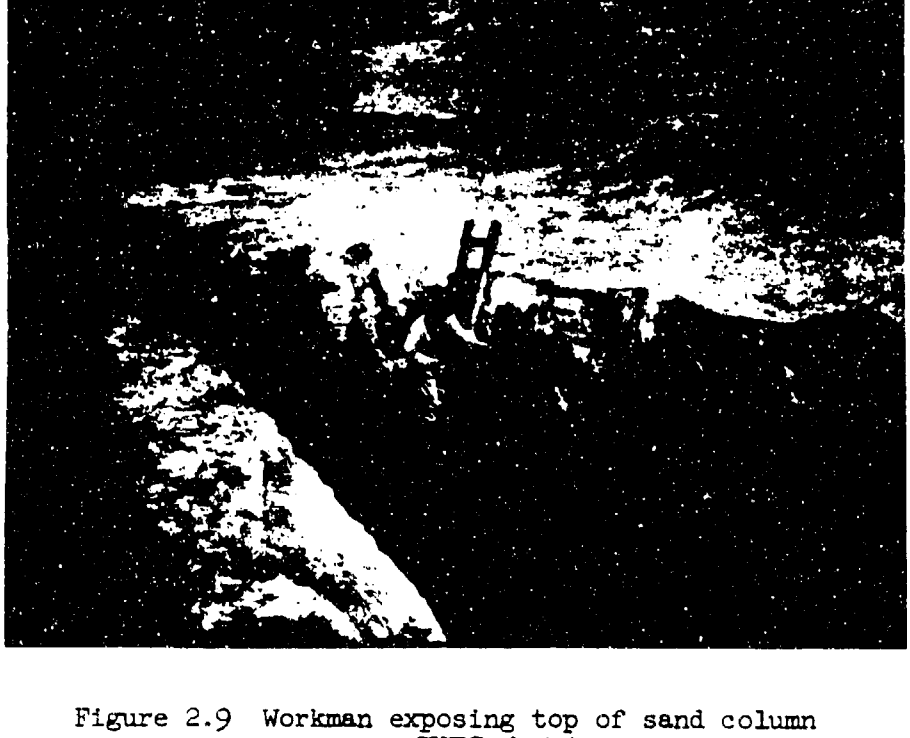

Figure 2.9 Workman exposing top of sand column 70 feet south of GZ. (WES photo)

Figure 2.10 Workman exposing lower portion of sand column 90 feet south of GZ. (WES photo)

CHAPTER 3

RESULTS

3.1 APPARENT CRATER MEASUREMENTS

Measurement of the Small Boy apparent crater was accomplished by stereocontouring from aerial photographs taken before and after the shot (Paragraph 2.4). Figures 3.1 and 3.2 are sample preshot and postshot aerial photographs; Figure 3.3 is a typical postshot stereopair; and Figures 3.4 and 3.5 are the preshot and postshot contour maps prepared from the aerial photographs. Figure 3.6 is a contour overprint of the crater. The average apparent crater radius derived from the contour maps was 180 feet, and the measured apparent crater depth at ground zero was 1.5 feet.

In general appearance, the crater was reasonably symmetrical in plan (excluding the area southwest of ground zero, which was influenced by other projects) but somewhat irregular in circumference. Its deepest point below original ground surface was The large mound in the center of the crater gives an apparent depth at ground zero which is not consistent with the overall appearance of the crater. A more representative depth of

was obtained by using the contour map to construct profiles along two crater diameters and extending the average crater profile slopes in to ground zero, which results in a profile that lies approximately 3 feet below the ground zero mound (Figure 3.7).

The apparent crater radius as scaled directly from the contour map may also be misleading. Because of rather wide variations in the crater radius, which stems from an inability to establish the point of intersection of the crater profile and the original ground surface, the average apparent crater radius was determined by measuring the area of the relatively undisturbed northeastern half of the apparent crater with a planimeter and solving the equation $r = \sqrt{A/\pi}$, where r is the crater radius, and A is the measured area.

It was planned to obtain profiles by conventional surveys when radiation levels permitted, but the area near ground zero had been disturbed to such an extent that profiles could be made only of the outer portion of the crater area. The survey was run along the sand-column diameter (approximately north 31 degrees west and south 31 degrees east); the resulting profile checked very closely with that scaled from the contour map.

3.2 MEASUREMENT OF THE TRUE CRATER AND ZONES OF DEFORMATION

3.2.1 Sand-Column Recovery. All of the sand columns emplaced in the Small Boy crater area were recovered in the postshot excavation. All were exposed in their entirety except the columns 5, 10, and 25 feet either side of ground zero. The columns 25 feet north and south and 5 feet north were recovered as far down as their deepest asphalt layers (35 feet), while those 10 feet north and south and 5 feet south were recovered to the 30-foot-deep asphalt layers. The columns were in excellent condition and appeared to have matched the strength and density of the surrounding soil so closely that virtually every permanent movement of the soil caused by the detonation was clearly reproduced in the colored sand columns (Figures 3.8 and 3.9). The postshot positions of the sand columns are shown in Figure 3.10.

3.2.2 True Crater Dimensions. The true crater resulting from the Small Boy event was found by locating the elevations above which the sand columns were no longer discernible. To ascertain the general configuration of the true crater, a smooth line was drawn through the tops of the sand columns in a profile view such as that shown in Figure 3.10.

Immediately underlying the central portion of the true crater was a highly deformed, shalelike material which by its burned appearance and extreme bedding convolutions gave clear evidence of the heat and pressure cycle that it had undergone. Upon excavation, this material sloughed away readily. Although it was considered as fallback, it had not experienced the type of dissociation usually associated with fallback found in a crater resulting from a buried shot.

In the outer regions of the crater, the true crater was assumed to be coincident with the apparent crater surface. The resulting dimensions were a true crater radius of

and a true crater depth of

3.2.3 Zone of Rupture and Shear. The rupture/shear zone is the most difficult zone of deformation to define, both in theory and in practice. The difficulty lies in determining the boundary line between small shears and ruptures in the rupture/shear zone and plastic movement in the plastic zone. In the Small Boy experiment, almost all horizontal movement was in the form of bedding-plane shears which probably coincided with sedimentary layers. The individual shears in the sand columns ranged in magnitude from more than 1 foot to as small as 0.01 foot and ranged in

vertical intervals from 2 or 3 feet to every 0.05 foot. The rupture/shear zone was arbitrarily limited to shears of at least 0.05 foot in magnitude; the resulting zone based on this limit is illustrated in Figure 3.7. Unfortunately, the rupture/shear zone near the ground surface extended much farther from ground zero than was anticipated and thus was well beyond the limits of the sand-column array. In addition to the subsurface evidence of rupture, the aerial photographs clearly showed concentric rupture rings to a distance of more than 150 feet from ground zero (Figures 3.2, 3.3).

3.2.4 Plastic Zone. The plastic movement of the soil medium in horizontal directions from ground zero was much less than expected. Horizontal plastic movement ranged from 0.5 foot at a depth of 23 feet in the sand column 10 feet south of ground zero to 0.1 foot of movement at a depth of 7 feet in the sand column 90 feet south of ground zero. Transverse horizontal movement of the columns (normal to the Project 1.9 array) was also measured, based on the preshot alignment of the column array. As might be expected, this phenomenon was apparently random in nature, with measured movements of up to 0.5 foot in various columns.

Downward plastic movement of the soil medium near ground zero was much greater than expected. The asphalt layers in the sand columns provided an excellent record of the magnitude and extent of the vertical movement. Actually, permanent vertical movement occurred at depths greater than the deepest asphalt layers but decreased in such a uniform manner that it was possible to estimate with reasonable confidence the depth at which plastic movement became insignificant. The vertical plastic movement, as recorded by the asphalt layers, ranged from immediately below the true crater near ground zero to at a depth of below the original ground zero elevation and for the lower portions of the columns 120 feet from ground zero.

3.3 SUMMARY OF CRATER MEASUREMENTS

Table 3.1 contains a summary of Small Boy crater measurements, including values scaled according to $Y^{1/3.4}$-scaling. Volumes in this table are based upon assumed conical shapes for the apparent and true craters, with adjustments being made for departures of the crater profiles from this general shape.

Page 48
Deleted

Figure 3.1 Preshot aerial photograph of the Small Boy crater area. GZ can be identified by extending the tic marks until they intersect. (WES photo)

Pages 50-51
Deleted

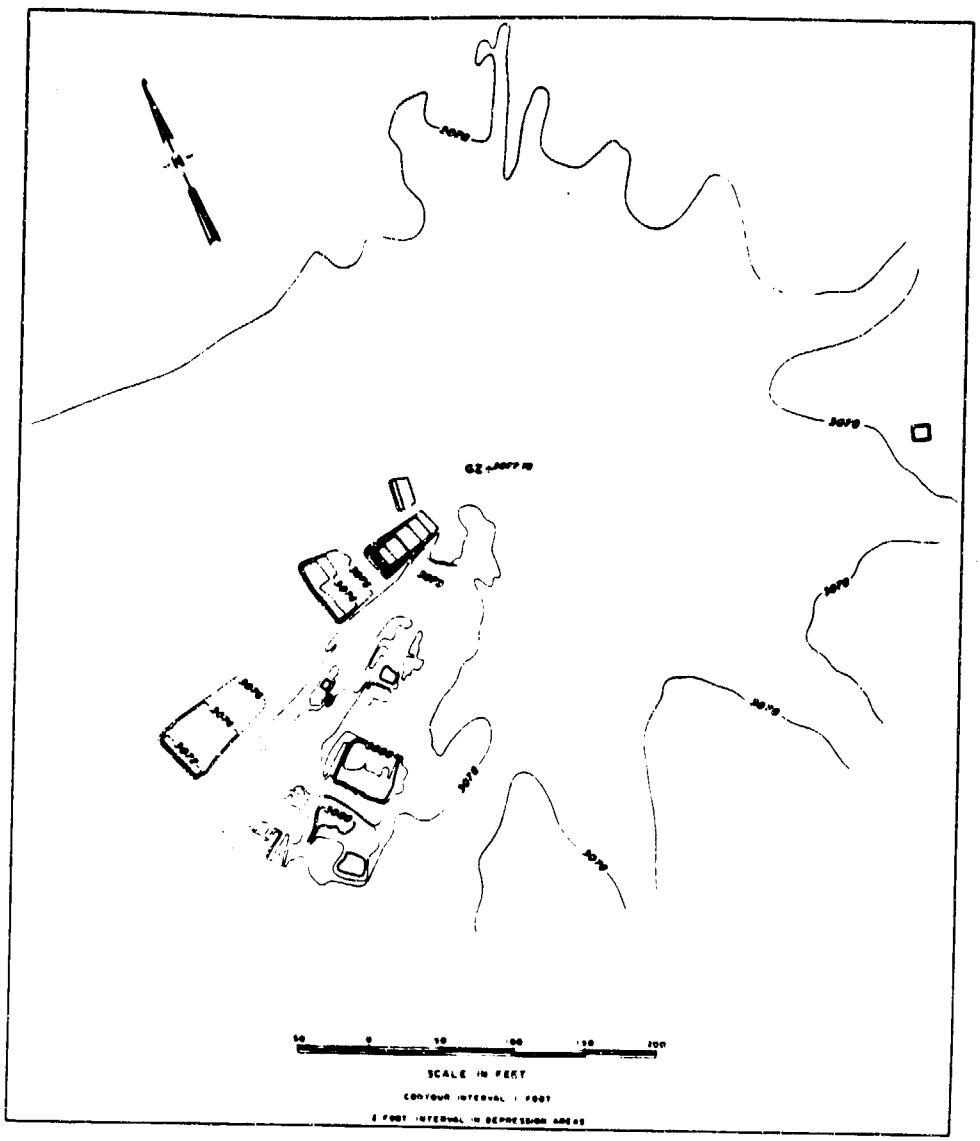

Figure 3.4 Preshot contour map of Small Boy crater area.

Pages 53-55 Deleted

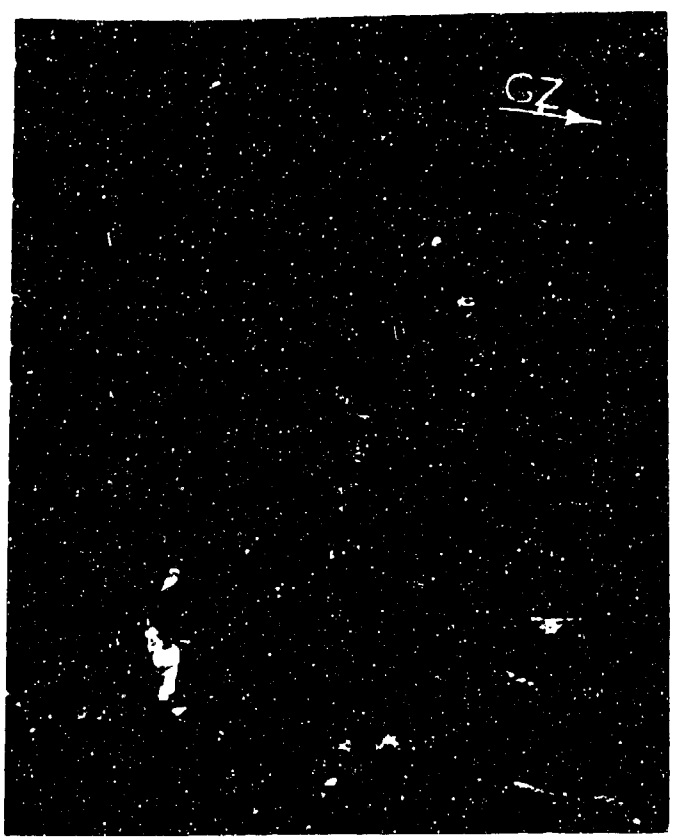

Figure 3.8 Recovered sand column 90 feet north of GZ. **(WES photo)**

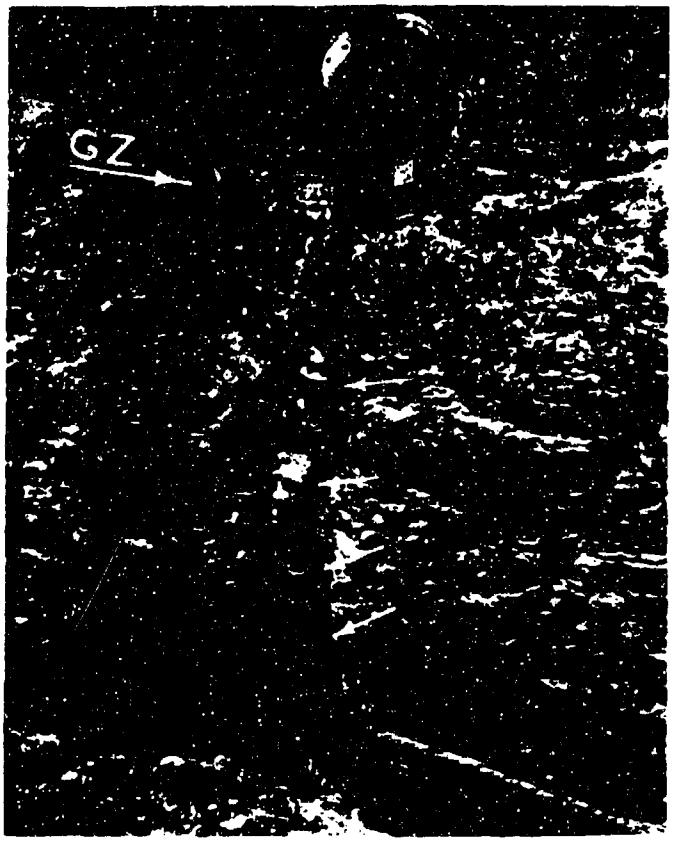

Figure 3.9 Recovered sand column 120 feet north of GZ. Arrows indicate asphalt layers. **(WES photo)**

Page 58 Deleted

CHAPTER 4

DISCUSSION

4.1 DATA RELIABILITY

4.1.1 Apparent and True Crater Measurements. Profiles of the Small Boy apparent crater were initially made from aerial stereophotograph contour maps, with vertical accuracy estimated at ±0.5 foot. As mentioned previously, the apparent crater from ground zero was disturbed by work on another project before a conventional survey of the crater could be made. However, one diameter of the apparent crater beyond the disturbed zone was surveyed, and the data checked closely with that from the aerial map. True crater measurements were made by conventional survey methods after the first stage of excavation of the sand-column trench had been completed. No unusual problems were encountered, and the data thus obtained are considered highly reliable.

4.1.2 Sand-Column Recovery. The sand columns were in excellent condition when exposed (see Figures 3.8 and 3.9), although the explosion had caused severe rupture and shear of the material near the ground surface. A detailed visual

inspection of the trench wall containing the exposed columns gave no evidence of discontinuities between the columns and the surrounding soil. The matching of strength, moisture content, hardness, and bonding of the columns with the soil medium appeared excellent.

4.2 ANALYSIS OF RESULTS

The analysis of the data from the Small Boy crater is discussed herein in terms of five characteristic boundaries and response zones which comprised the crater, i.e. the apparent crater, the true crater, the rupture and shear zones (combined in Small Boy), and the plastic zone. The elastic zone is not discussed since no permanent deformation occurs in this region wherein all explosion-induced motions are elastic (no net displacement follows the passing of the transient loads). The four major response zones that experienced permanent deformation are discussed hereafter in reverse order (from bottom to top of the crater) in order to better follow the continuity of their formation.

4.2.1 Plastic Movement. The Small Boy event afforded a unique opportunity to study plastic movement in a homogeneous soil medium resulting from a very large dynamic

loading. Comparisons of the preshot and postshot positions of the asphalt layers emplaced in the sand columns indicate that measured vertical plastic movement in the columns ranged from 1 to 50 times as much as horizontal movement for individual asphalt layers. Figure 4.1 shows the relative magnitude and direction of permanent displacement of the soil medium by presenting plots of preshot and postshot soil positions. There was almost no horizontal movement of a plastic nature, i.e. soil flowage; the movement in the upper regions of the zone was attributed to horizontal shearing. The small amount of horizontal displacement that can be considered plastic occurred in insignificant amounts in the lower portions of the columns near ground zero and was in the form of a very slight bowing toward the ground zero axis. Some slight, random, horizontal movement also occurred normal to the axis of the sand columns but did not exhibit any apparent pattern.

The attenuation of permanent vertical displacement with both horizontal and vertical distance from ground zero was remarkably uniform. Figure 4.2 is a cross-sectional profile of the soil medium along the sand-column axis. The contours indicate the permanent vertical displacement of the sand

columns versus their depth and range from ground zero and are plotted from the preshot and postshot elevations of the asphalt layers. Figures 4.3 and 4.4 are semilogarithmic plots of depth versus permanent displacement for sand columns 120, 50, and 25 feet from ground zero. A similar plot (Figure 4.4) for a theoretical column beneath ground zero is based on extensions of the contours of Figure 4.2. Data points plotted on these graphs are the average values for columns equal distances north and south of ground zero Extensions of the curves in Figures 4.3 and 4.4 indicat that permanent vertical displacement decreased to less than 0.5 foot at a depth of approximately 70 feet below ground surface at ground zero and at a depth of approximately 13 feet below ground surface 120 feet from ground zero. An interesting discussion of the relation of overstress to overburden stress, as it affects vertical movement in soil, is contained in Reference 11 where it is postulated that below a depth of about 80 feet, the overstress-overburden stress ratio resulting from such a dynamic load rapidly approaches unity, and residual vertical deformation decreases accordingly.

If the individual sand columns beneath the Small Boy

crater are considered as a series of unit lengths (the distance between asphalt layers being one unit), then an average strain can be computed for each unit length along the columns. Figure 4.5 is a plot of percent compression per unit length (strain) of sand column versus depth below ground surface at ground zero, and Figure 4.6 is a similar plot of percent compression versus horizontal distance from ground zero at two selected depths (15 and 10 feet) below the preshot ground surface.

During the sand-column excavation, two soil density samples were taken from the plastic zone for comparison with preshot soil densities; one was extracted from a depth of 36 feet below ground zero (Figure 4.5) and the other from just below the true crater 30 feet from ground zero (Figure 4.6). Results of the tests showed increases in density of approximately 15.7 percent just below the true crater and 10.5 percent at the 36-foot depth (Reference 12). These results compare very favorably with the compression shown by the curves in Figures 4.5 and 4.6.

4.2.2 Soil Rupture and Shear. By far the greater portion of the Small Boy rupture/shear zone consisted of regular horizontal shears, particularly in the sand columns more

than 25 feet from ground zero. Almost all of the shear displacements occurred in the direction of ground zero; this oddity resulted from elastic rebound. To clarify this, consider a small element of soil located just below the ground surface at some horizontal distance from ground zero. At some finite time t_1 after detonation, the peak stress wave strikes the soil element. The element is then displaced in the direction of the applied force (away from ground zero) by elastic compression of the element itself and other elements beyond it. At some later time t_2, when the peak stress wave has passed beyond the soil element, a force is exerted upon the element in the direction toward ground zero to balance the sum of the pressures surrounding it. This force (assisted by the elastic expansion of the element and others beyond it after release of the initial shock-wave pressures) displaces the soil element back toward ground zero. However, during the milliseconds that elapsed during this phenomenon, a crater was formed and the horizontal confinement of the element was reduced in the direction of ground zero. Hence, the element is free to move permanently (by shearing) toward ground zero. This phenomenon is, of course, influenced by the physical structure and properties

of the medium and has been observed previously in fine-grained, cohesive soils (References 13 and 14).

The average size of the horizontal shears in the crater decreased only slightly with depth along the individual sand columns, until some depth was reached at which during the explosion the horizontal stresses were less than the shear strength of the columns, and shearing ended abruptly. However, horizontal displacement decreased rapidly with depth, since the total horizontal displacement of an element of soil was the sum of the individual shears and, in some cases, the plastic flow that occurred.

The area labeled "rupture/shear zone (severe)" in Figure 3.7 is that region in which crushing, pulverizing, and severe horizontal shearing toward ground zero occurred in the sand columns. In the area labeled "rupture/shear zone (moderate)," there was little or no crushing of the columns, and horizontal movement was primarily limited to small shears (0.1 foot or less).

It is recognized that the classification of these zones differs from those previously used, and further, that the configuration of the rupture/shear zone (or zones) will vary with burst geometry. Much of the shallow, subsurface

deformation surrounding a true crater, which has heretofore been classified as "plastic zone," is actually attributable to a combination of shearing and plastic movement. A region which has undergone primarily vertical plastic movement may lie beneath a region wherein some shear has occurred, as was the case in the Small Boy event. Division of these zones thus becomes rather arbitrary, since two or more of these phenomena often coexist. In the Small Boy crater area, the zone of shear failure in the outlying sand columns and the closer-in zone in which fracture, or rupture, of the columns predominated formed a continuous region which is referred to as the "rupture/shear" zone, since both designations describe breaking or sliding, rather than flowing, of the medium. This zone probably does not occur with buried shots, where plastic flow completely surrounds the crater and creates a region of upthrust at the ground surface. In such a case, the zone of extreme fracturing (rupture) will probably closely envelop the true crater boundary, and a zone in which shear predominates may occur near ground surface at a distance beyond that of plastic flow. Unless the results of a specific phenomenon are desired, all such zones beneath and beyond the true crater can be considered to be within the

envelope of permanent (plastic) deformation (Figure 1.1).

4.2.3 True Crater. Extension into ground zero of a smooth curve connecting the tops of the sand columns shows the true crater depth at that location to approximate feet, which correlates closely with visual examination of the side of the trench. From Figure 4.2, the residual vertical displacement at ground zero can be plotted, as shown in Figure 4.4, as a function of presnot depth. Extrapolation of this curve to original ground surface indicates a total permanent displacement of but this does not account for such phenomena as spalling due to elastic rebound, vaporization, scouring, etc. In other words, if it had not been ejected, the original ground surface might have undergone a plastic compression of As it was, the identifiable true crater surface exhibited a downward displacement of about Thus, 55 percent of the true crater depth at ground zero is attributable to compression. It is believed that no reliable estimate of total displacement (maximum transient) can be made from the data available. That which might be inferred from laboratory tests (Reference 11) seems unreasonably high in this case.

By using the curves in Figures 4.3 and 4.4 to estimate

the permanent vertical displacement of the remaining surface of the true crater, it was found that roughly 60 percent of the true crater volume was the result of plastic compression. The remainder of this volume must be due to the scouring action of the expanding fireball and gases, ejecta carried aloft and deposited beyond the crater by wind and base surge, and vaporization of the medium.

Immediately above the true crater there was a zone of substantial thickness (~12 feet at ground zero) wherein the material appeared to have been dissociated from the in situ mass below it without having become involved in the throwout or dirt stem resulting from the updraft and afterwinds. It should be noted that although the true crater surface is that above which the medium is completely dissociated, the true crater depth and the depth of the in situ soil which was completely dissociated are two different dimensions, the latter not including plastic compression.

Figure 3.7 shows a distinct depression in the bottom of the true crater which is not continuous with the overall true crater surface. The depression extends out horizontally to a distance of approximately feet from ground zero; the profile in this area appears to be

concentric about the point of burst. This bulb is believed to reflect the effects of the kinetic energy of the device debris and vaporization of material which occurred in the immediate vicinity of ground zero early in the time history of the explosion (Reference 15).

4.2.4 Apparent Crater. The volume of the Small Boy apparent crater seems largely attributable to the permanent compression of the underlying medium. The true crater configuration indicates a volume of about cubic yards, but it appears that only about 40 percent

is due to vaporization or ejection of in situ material, as explained in Paragraph 4.2.3. Since fallback within the crater amounted to about

yards, the Small Boy event probably would have produced a convex rather than a concave crater if it had not been for the permanent compression of the soil beneath the true crater surface. The unusual composition of the fallback was noted in Paragraph 3.2.2.

The foregoing conclusion is based on the assumptions that a very small percentage of material was ejected or carried aloft by the explosion, and that the disturbed fallback occupied a volume approximately 30 percent greater than

it occupied in its in situ condition. The mound which aerial photography shows as having been near ground zero is believed to have resulted from elastic rebound and deposition of fine material by the afterwinds and by fallback from the dirt stem beneath the fireball.

4.3 CORRELATION WITH PREVIOUS DATA

4.3.1 General Cratering Relations. As discussed in Paragraph 1.4, experiments have indicated that a scaling relation exists between cratering parameters that is approximately proportional to the 1/3.4 power of the yield (or TNT equivalent weight) in the range of yields which includes the Small Boy event. Figures 4.7 and 4.8 are plots of apparent crater dimensions versus depths of burst (DOB) for cratering events in NTS alluvium, based on the scaling of these values according to $kt^{1/3.4}$ (Reference 15). The curves are drawn to favor the larger yields (> 5 tons), although data points are included for all cratering shots having yields greater than 256 pounds.

4.3.2 Comparison with Other Near-Surface Cratering Events. Table 4.1 is a compilation of crater data for large-yield (> 5 tons) cratering events which were low air,

surface, or shallow underground bursts. Figures 4.9 and 4.10 are plots of scaled apparent and true (when available) crater dimensions versus scaled HOB or DOB from Table 4.1. The left portions of the two graphs are merely extensions of the curves of Figures 4.7 and 4.8.

Despite some differences in the cratered media, the data points for scaled crater depths versus DOB(HOB) form a fairly smooth curve. Note that the Small Boy apparent crater depth falls at the minimum point of the curve in Figure 4.9, indicating that a slightly lower HOB would have greatly increased the apparent depth, while a higher HOB would have only slightly decreased the apparent depth. While insufficient data are available from which to construct true crater curves, it appears that the true crater depth is somewhat more sensitive to burst geometry in this region.

In the plot in Figure 4.10, there is considerable data scatter, particularly for scaled HOB's just above the surface. Although the minimum point of the curve seems well defined, the location of the steep portion of the curve left of the minimum point is somewhat indefinite.

The shape of the curve in Figure 4.10 is actually due to the presence or absence of a conventional crater side

slope and lip, which in turn is dependent primarily upon the HOB. If a nuclear device were detonated over a flat, homogeneous medium at an arbitrarily selected HOB of 3 $ft/kt^{1/3.4}$, the resulting crater would resemble that of Figure 4.12a. The radius of the apparent crater would be the horizontal distance between ground zero and the intersection of the original ground elevation with the interior slope of the crater. If, however, the HOB were increased to perhaps 20 $ft/kt^{1/3.4}$, the resulting crater would resemble that shown in Figure 4.12b. The apparent crater radius then becomes the horizontal distance from ground zero to the intersection of the original ground elevation with the postshot ground surface. As may be seen in the profiles in Figure 4.12, the apparent crater radii for the two types of craters are totally different. Very likely, the minimum point on the curve of Figure 4.10 represents the point of transition between the two types of craters.

It is evident from the curve in Figure 4.10 that the radius of the Jangle S crater (data point 10) was measured in the manner specified for the type crater shown in Figure 4.12a, while the Small Boy and Trinity crater radii (data points 13 and 14) were measured according to measuring

specifications for the type crater shown in Figure 4.12b. Note that the crater radii for the two Little Feller craters (data points 2 and 7) fall almost directly on the minimum point of the curve in Figure 4.10. These points may, however, be slightly to the left of their correct position, due to the influence of such unscaled factors as the strength, density, and homogeneity of the medium.

Since volume is simply a function of radius and depth, the curve in Figure 4.11 is a combination of the data shown in Figures 4.9 and 4.10.

Pages 74 - 85
Deleted

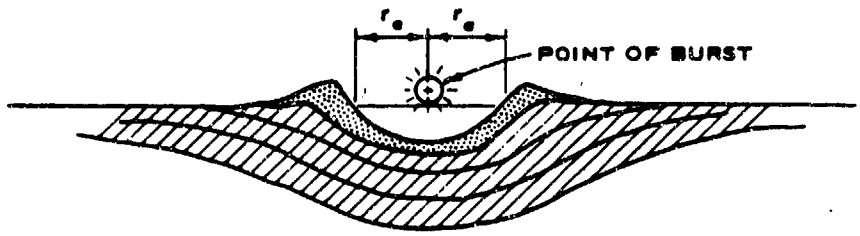

a. Conventional crater.

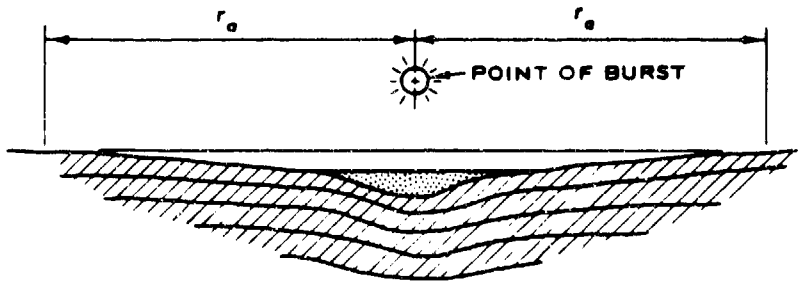

b. Compression crater.

Figure 4.12 Apparent crater radii for two types of craters resulting from low airbursts.

CHAPTER 5

CONCLUSIONS AND RECOMMENDATIONS

5.1 CONCLUSIONS

In Small Boy Project 1.9, a relatively uncomplicated and inexpensive experiment yielded much valuable information concerning the mechanics of crater formation resulting from low airbursts. An obvious limitation inherent in the use of sand columns is that the only record provided is the finished crater; the process of its formation can only be inferred. However, there is no other method known to the authors which so completely and reliably documents the crater shape and defines the extent and direction of residual motion.

Comparative plots of the Small Boy crater dimensions with those of other craters in NTS alluvium and similar media showed few differences, although the medium in Frenchman Flat differs rather markedly from that in other shot locations.

From a comparison of the Small Boy cratering results with those of previous near-surface events, it appears obvious that there is a critical range of burst heights

which effect a distinct change in the configuration of the crater. This critical region represents the burst height at which the energy coupled between the device and the medium is so diminished by the intervening airspace that the crater is changed from one primarily formed by ejection of in situ material to one formed principally by plastic flowage and compression of the material. Before this critical point is reached, the general characteristics of the crater are similar to those of craters formed by shallow underground explosions. At burst heights slightly above the critical (Figures 4.9 through 4.11), the following changes in the nature of the crater become apparent:

1. Apparent crater radius increases rapidly with small increases in HOB, and apparent crater depth decreases only slightly with increasing HOB ($0 < HOB < 50$).

2. True crater radius becomes coincident with the apparent crater radius.

3. A considerable amount of material within the true crater is dissociated from the in situ material by elastic rebound phenomenon.

4. There is virtually no throwout from the

crater, and no crater lip is formed.

5. The volume of the apparent crater is primarily due to the permanent compression of the underlying medium. Evidences of these phenomena were found in Small Boy.

Other phenomena observed in the Small Boy experiment, but which were not necessarily a part of the transition between crater types, were:

1. Permanent vertical soil displacement was much greater than expected, varying as a semilogarithmic function of depth for a homogeneous medium.

2. Extreme horizontal shearing occurred as a result of shock and elastic rebound near the ground surface.

The conclusions drawn from the Small Boy crater investigation indicate that craters created in dry terrain by a nuclear airburst with an HOB greater than the critical point (10 ft/kt$^{1/3.4}$) will not constitute a tactical obstacle (excluding radiation effects), and the effects of throwout will be negligible. Damage to underground structures from a low airburst would likely result from the severe elastic and plastic compression in the ground zero area rather than from cratering per se.

5.2 RECOMMENDATIONS

It is vitally necessary, from a military standpoint, that sufficient data be acquired to quantitatively predict the cratering and subsurface effects of low-airburst nuclear explosions. Although considerable effort has been directed toward the investigation of craters formed by underground explosions, there is a drastic shortage of information relating to the cratering capabilities of near-surface explosions. Every opportunity should be taken to derive all possible information from events which will permit further definition of these phenomena in various media. The continued and expanded use of sand columns should aid in such studies.

REFERENCES

1. O. Richmond; "Preliminary Results of a Study on the Partition of Work from Explosives in Partially Confined Configurations"; January 1954; U. S. Army Engineer Research and Development Laboratories, Fort Belvoir, Virginia; Secret.

2. B. Perkins, Jr.; "A New Technique for Studying Crater Phenomena"; Technical Note 880, March 1954; U. S. Army Ordnance Ballistics Research Laboratory, Aberdeen, Maryland; Unclassified.

3. "Capabilities of Atomic Weapons"; Department of the Army Technical Manual 23-200, November 1957 (Revised Edition); U. S. Government Printing Office, Washington, D. C.; Confidential.

4. J. N. Strange, C. W. Denzel, and T. I. McIane III; "Cratering from High Explosive Charges, Analysis of Crater Data"; Technical Report No. 2-547, Report No. 2, June 1961; U. S. Army Engineer Waterways Experiment Station, Vicksburg, Mississippi; Unclassified.

5. M. D. Nordyke; "On Cratering. A Brief History, Analysis, and Theory of Cratering"; UCRL 6578, 22 August 1962; University of California Lawrence Radiation Laboratory, Livermore, California; Unclassified.

6. "The Effects of Nuclear Weapons"; Department of the Army Pamphlet No. 39-3, April 1962; United States Atomic Energy Commission; Unclassified.

7. H. G. Snay; "The Scaling of Underwater Explosion Phenomenon"; NOLTR 61-46, January 1962; U. S. Naval Ordnance Laboratory, White Oak, Maryland; Unclassified.

8. A. H. Barnes, J. N. Strange, and F. A. Pieper; "Effects of Explosions in Shallow Water"; Final Report, Technical Memorandum No. 2-406, April 1955; U. S. Army Engineer Waterways Experiment Station, Vicksburg, Mississippi; Unclassified.

9. L. J. Vortman; "Implications of Experimental Data on the Scaling of Crater Dimensions"; Bulletin No. 32, Shock, Vibration and Associated Environments, Protective Construction, Part II, August 1963; Office of the Director of Defense Research and Engineering, Washington, D. C.; Unclassified.

10. A. B. Vesic and R. D. Barksdale; "Theoretical Studies of Cratering Mechanisms Affecting the Stability of Cratered Slopes"; 30 September 1963; Engineering Experiment Station, Georgia Institute of Technology, Atlanta, Georgia; Unclassified.

11. S. D. Wilson and E. A. Sibley; "Ground Displacements Resulting from Air-Blast Loading" (unpublished); February 1962; Unclassified.

12. T. B. Goode and A. L. Mathews; "Soil Survey and Materials Control"; Project 1.8, Operation Sun Beam; POR (WT) 2207, April 1963; U.S. Army Engineer Waterways Experiment Station, Vicksburg, Mississippi; Confidential.

13. G. H. S. Jones and J. E. Krohn; "Ground Displacement Near the Detonation of a 40,000-lb Hemisphere of TNT"; Technical Paper No. 213, 14 December 1960; Suffield Experimental Station, Ralston, Alberta, Canada; Unclassified.

14. J. M. Pinkston, Jr., and J. N. Strange; "Crater Measurements from a 100-Ton Surface Explosion"; Miscellaneous Paper No. 2-529, October 1962; U. S. Army Engineer Waterways Experiment Station, Vicksburg, Mississippi; Unclassified.

15. H. L. Brode and R. L. Bjork; "Cratering from a Megaton Surface Burst"; RM-2600, 30 June 1960; Rand Corporation, Santa Monica, California; Unclassified.

16. A. D. Rooke, Jr., and J. N. Strange; Little Feller I and II Project 1.9: Crater Measurements" (in publication); U. S. Army Engineer Waterways Experiment Station, Vicksburg, Mississippi; Secret.